Supplementary Material

Electrocatalysis as an Efficient Alternative to Thermal Catalysis over PtRu Bimetallic Catalysts for Hydrogenation of Benzoic Acid Derivatives

Yan Du, Xiao Chen*, Weilin Shen, Huibin Liu, Min Fang, Jinxuan Liu, and Changhai Liang*

State Key Laboratory of Fine Chemicals & Laboratory of Advanced Materials and Catalytic Engineering, School of Chemical Engineering, Dalian University of Technology, Dalian 116024, China.

* Corresponding author. Fax: +86 411 84986353. E-mail: xiaochen@dlut.edu.cn (X. Chen), changhai@dlut.edu.cn (C. Liang)

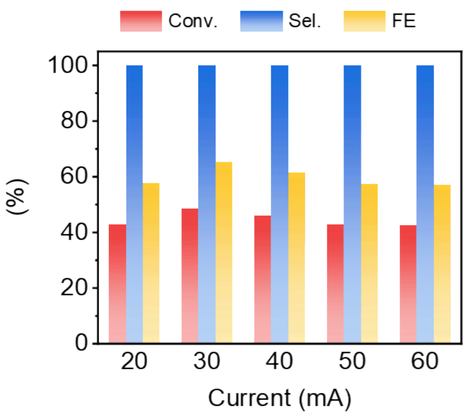

Figure S1. Conversion (Conv.) of BA, selectivity (Sel.), and Faradaic efficiency (FE) of CCA at various currents after consuming 108 charge.

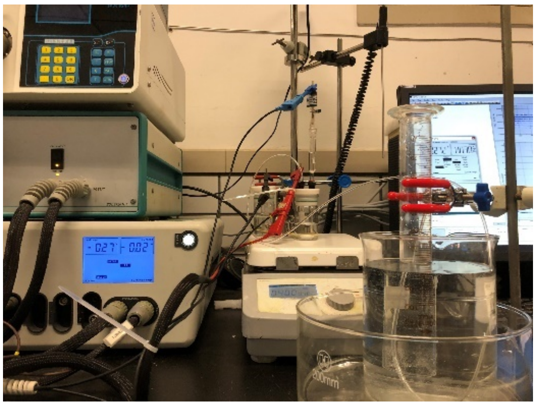

Figure S2. Schematic of the gas collecting device.

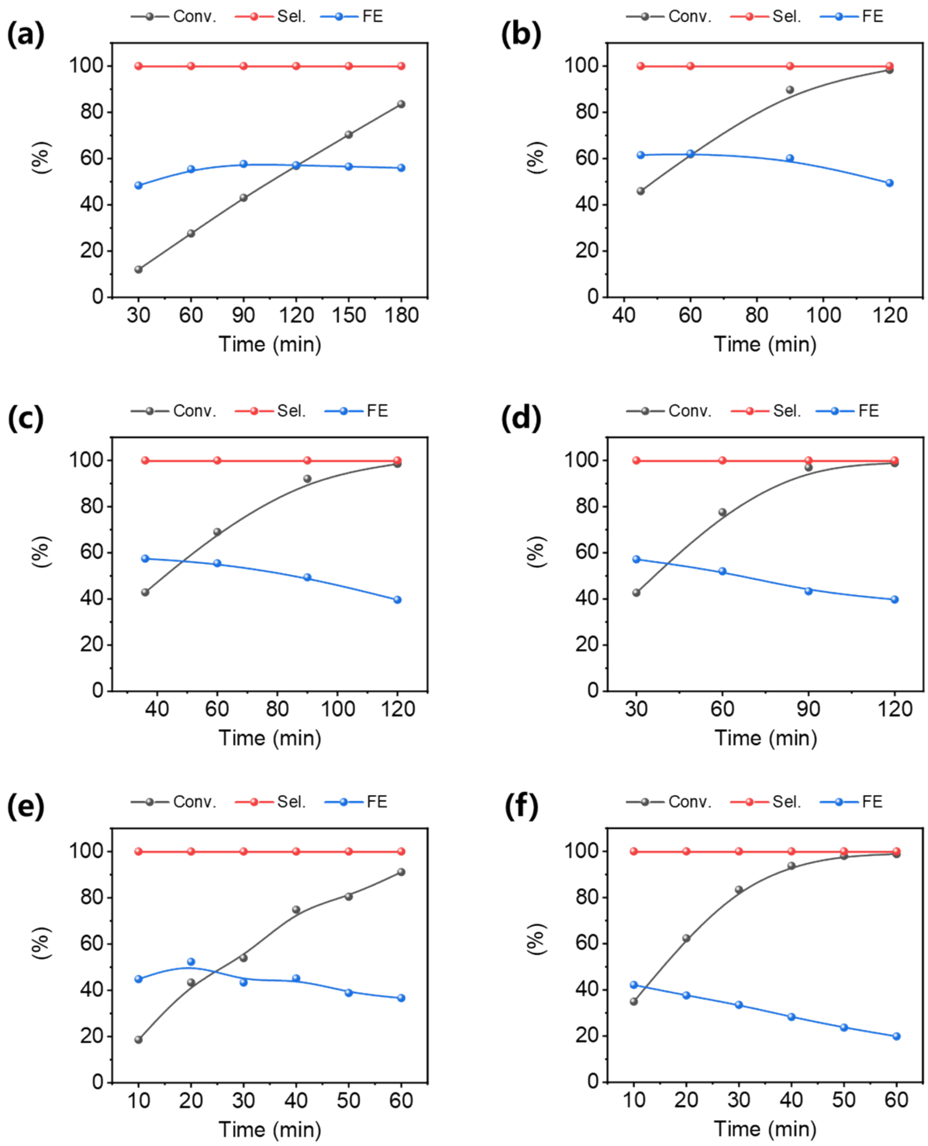

Figure S3. Conversion, selectivity, and FE for ECH of BA over PtRu/CP-4 at different reaction time under the current of (a) -20 mA, (b) -40 mA, (c) -50 mA, (d) -60 mA, (e) -100 mA, and (f) -200 mA.

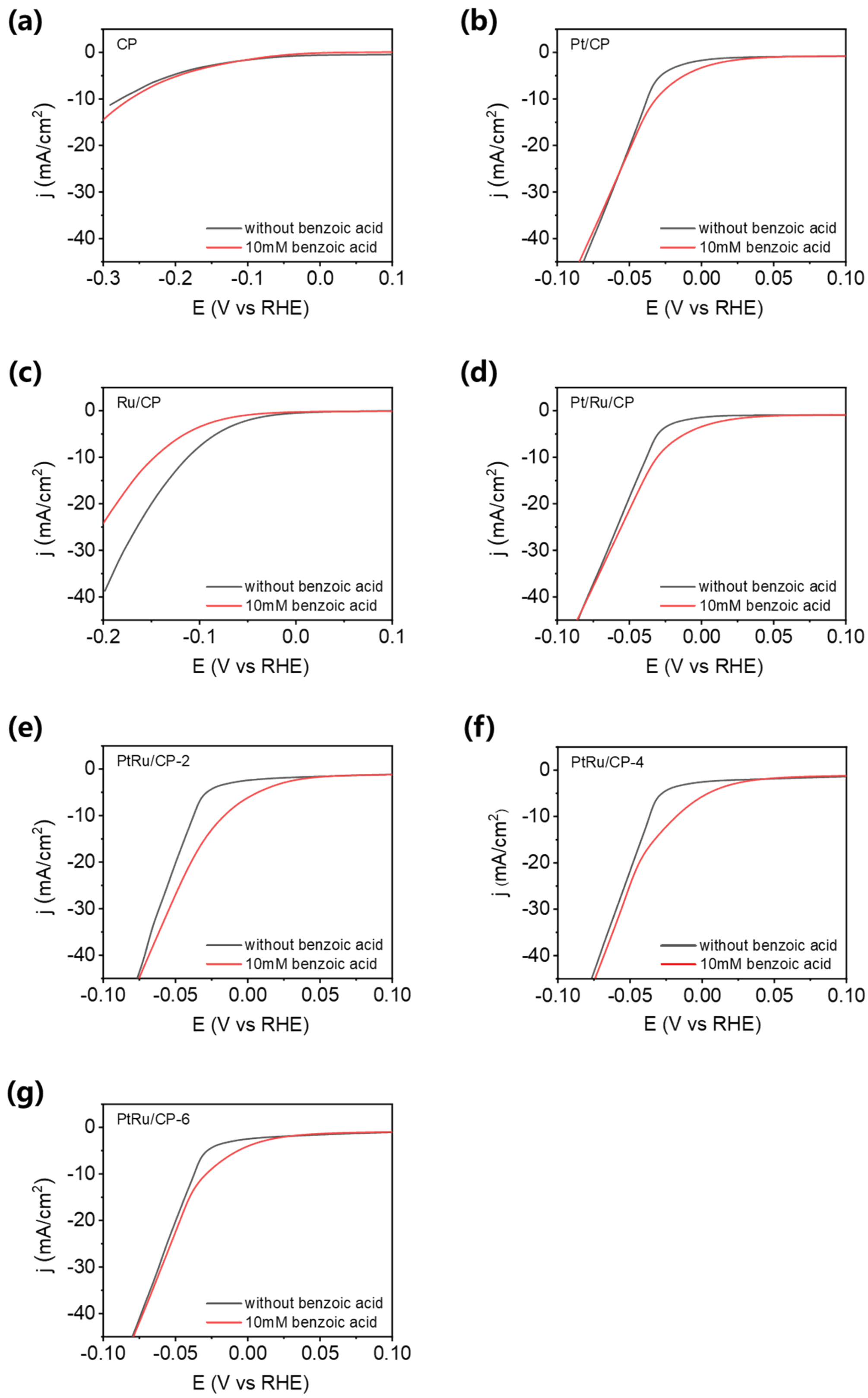

Figure S4. LSV (5 mV s^{-1}) curves of (a) CP, (b) Pt/CP, (c) Ru/CP, (d) Pt/Ru/CP, (e) PtRu/CP-2, (f) PtRu/CP-4 and (g) PtRu/CP-6 in 0.2 M H_2SO_4 with (red line) and without (black line) 10 mM BA.

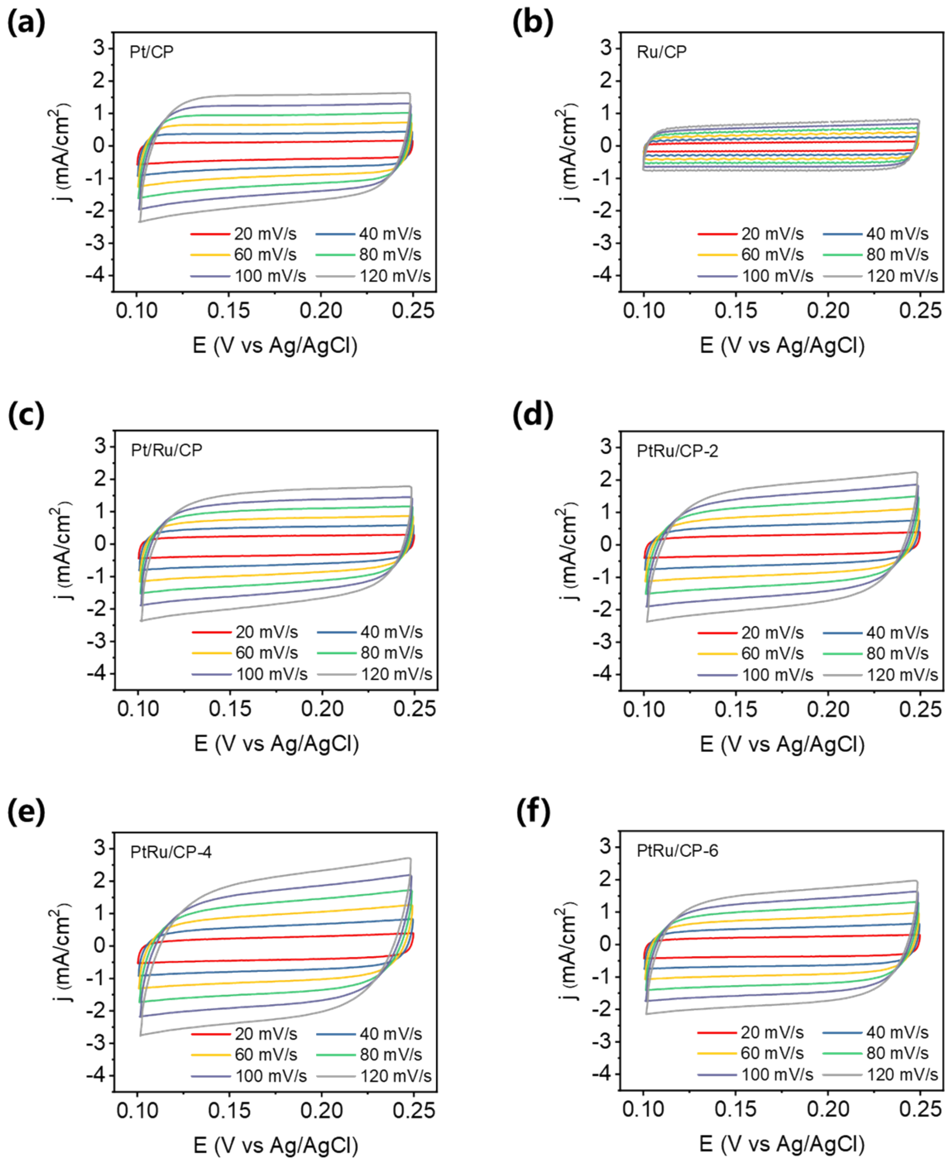

Figure S5. CV curves at various scan rates of (a) Pt/CP, (b) Ru/CP, (c) Pt/Ru//CP, (d) PtRu/CP-2, (e) PtRu/CP-4 and (f) PtRu/CP-6 in 0.2 M H_2SO_4.

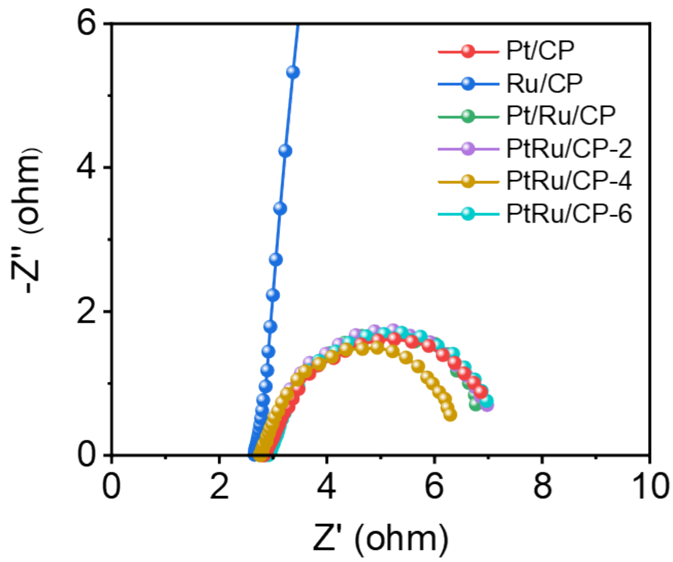

Figure S6. Nyquist plots for as-obtained electrocatalysts in 0.2 M H_2SO_4 with 10 mM BA.

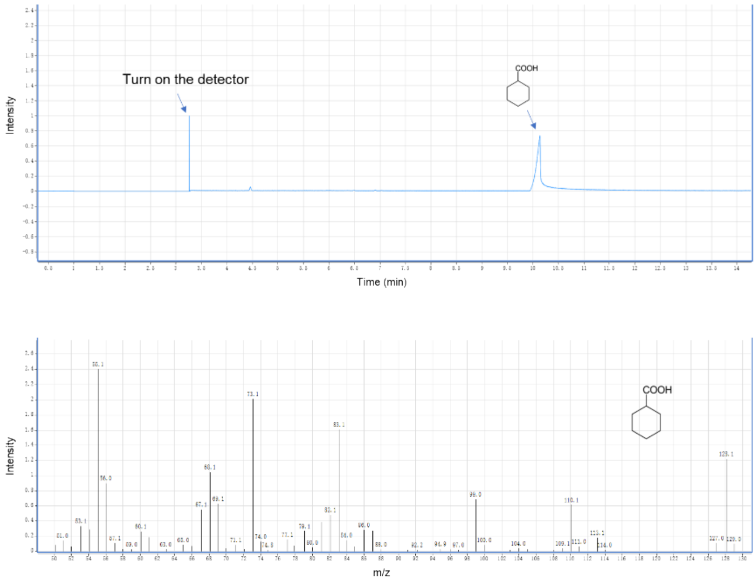

Figure S7. The original GC-MS spectra of products for ECH of benzoic acid.

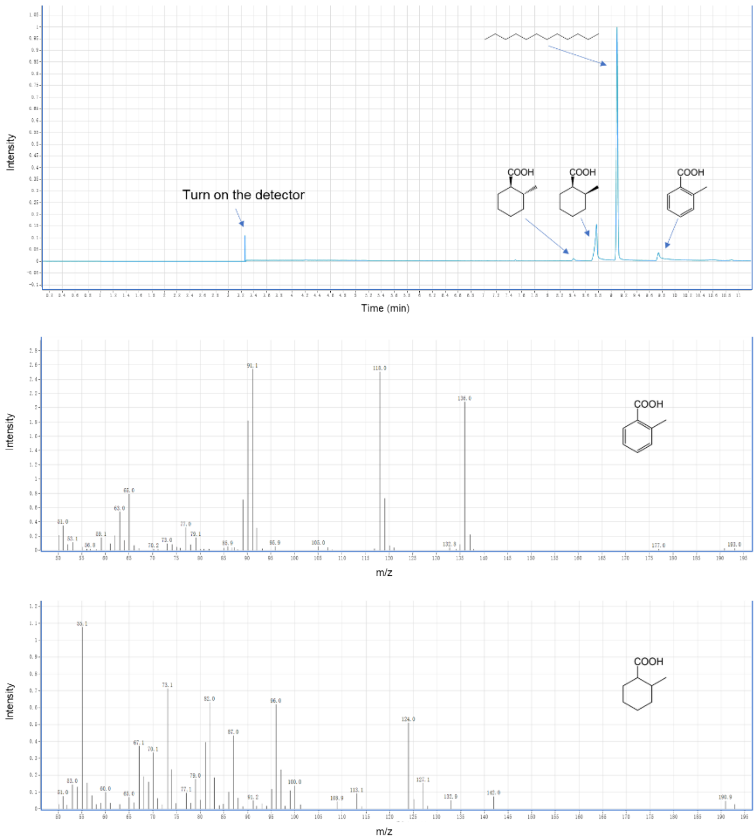

Figure S8. The original GC-MS spectra of products for ECH of *o*-methyl benzoic acid. (The extractant contains internal standard *n*-dodecane)

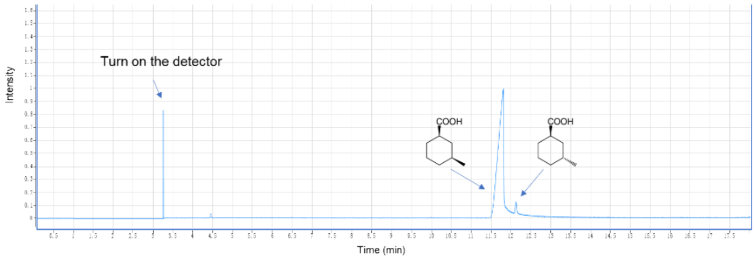

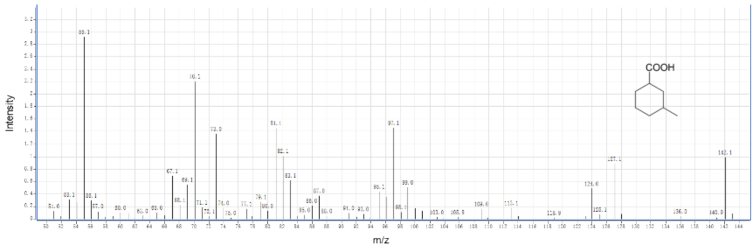

Figure S9. The original GC-MS spectra of products for ECH of *m*-methyl benzoic acid.

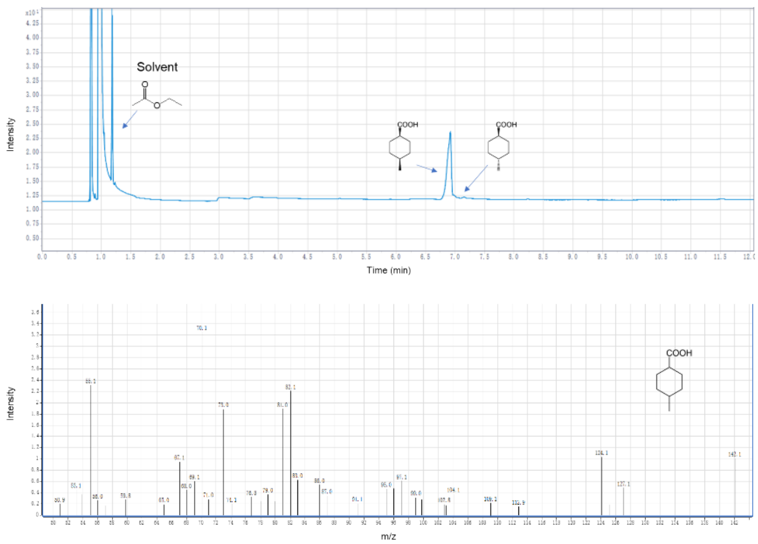

Figure S10. The original GC-MS spectra of products for ECH of *p*-methyl benzoic acid.

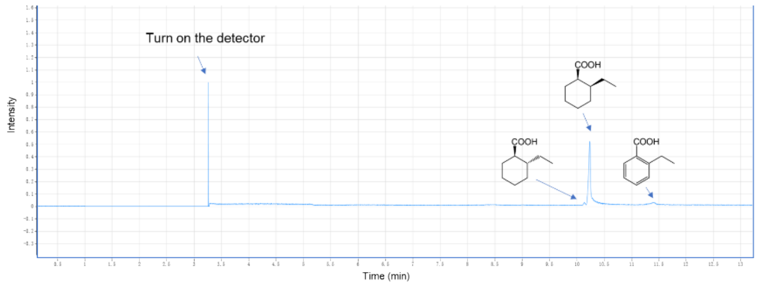

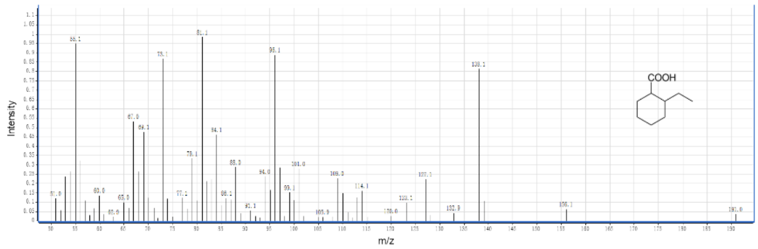

Figure S11. The original GC-MS spectra of products for ECH of *o*-ethyl benzoic acid.

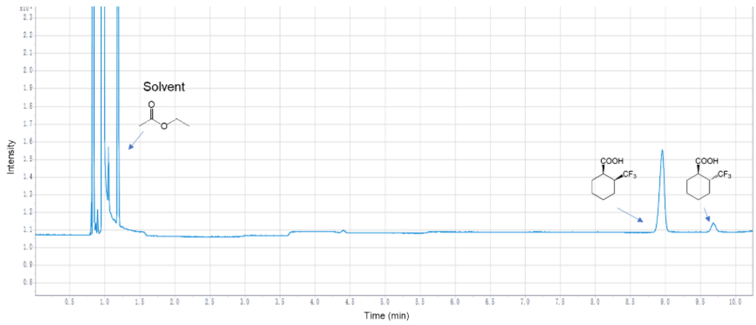

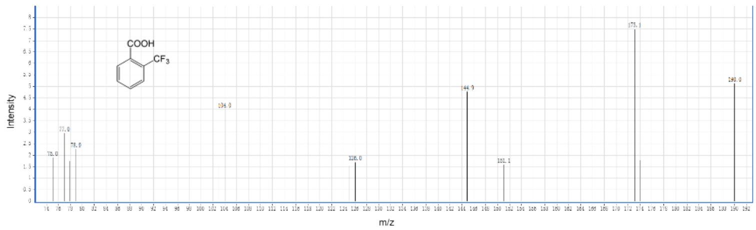

Figure S12. The original GC-MS spectra of products for ECH of *o*-trifluoromethylbenzoic acid.

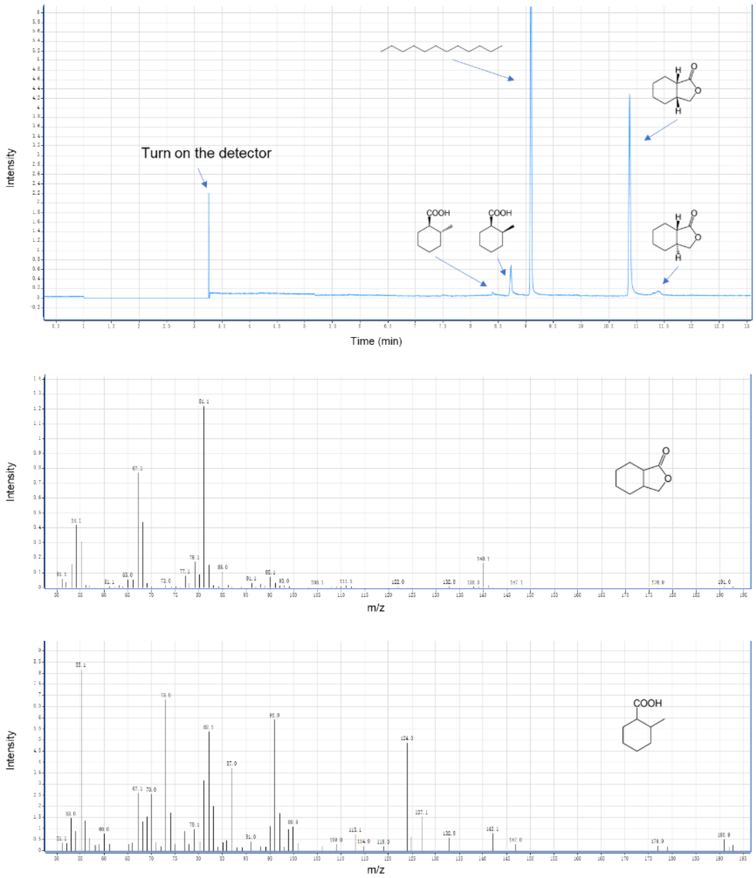

Figure S13. The original GC-MS spectra of products for ECH of phthalide. (The extractant contains internal standard *n*-dodecane)

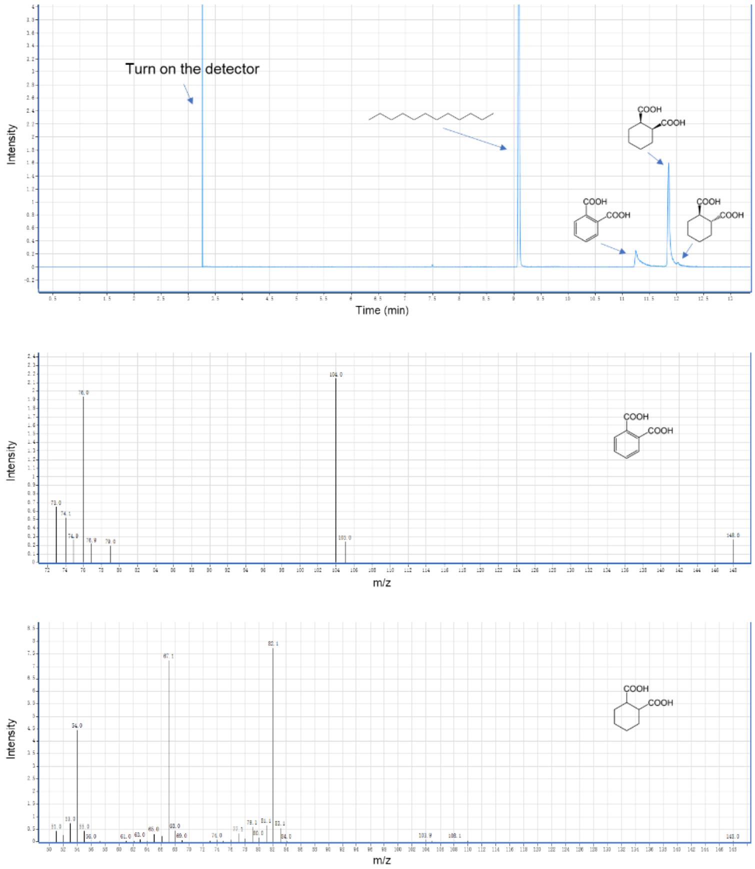

Figure S14. The original GC-MS spectra of products for ECH of phthalic acid. (The extractant contains internal standard *n*-dodecane)

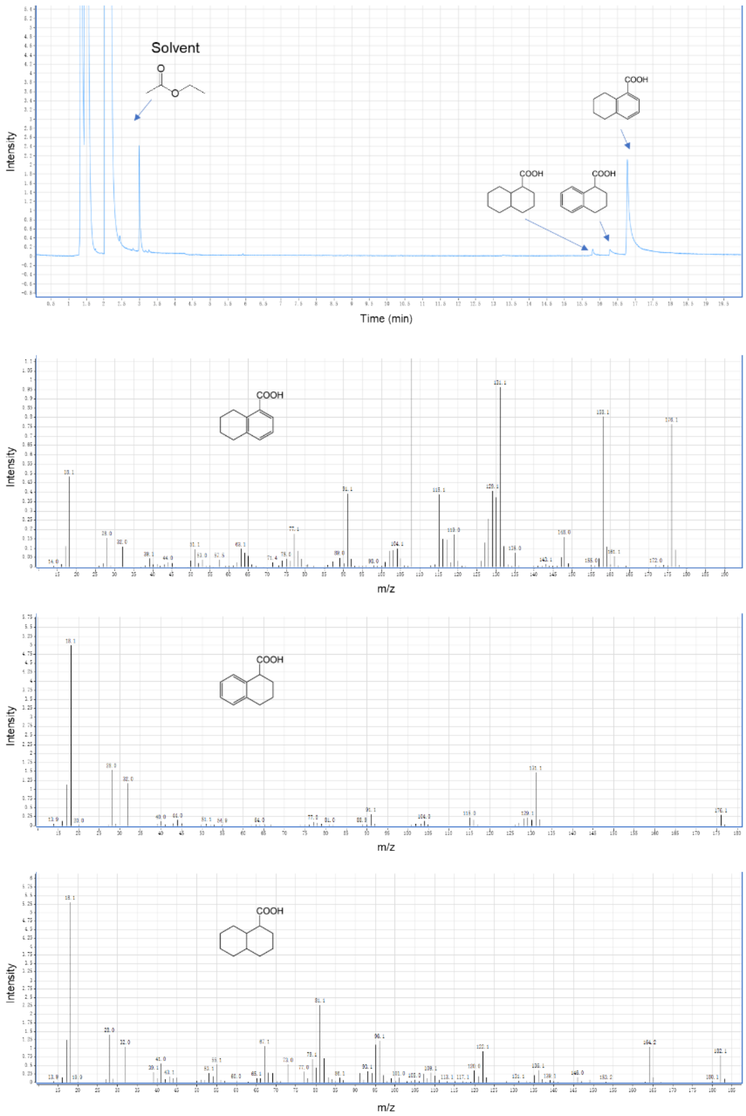

Figure S15. The original GC-MS spectra of products for ECH of 1-naphthoic acid.

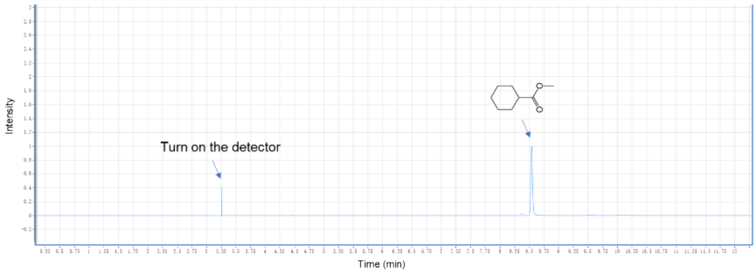

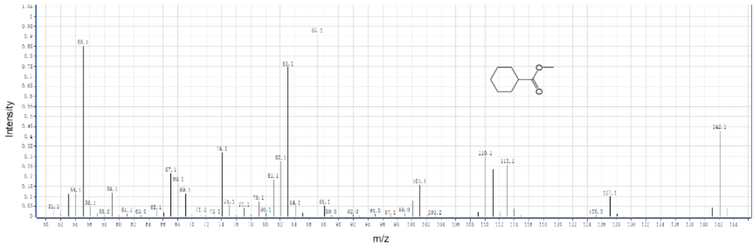

Figure S16. The original GC-MS spectra of products for ECH of methyl benzoate.

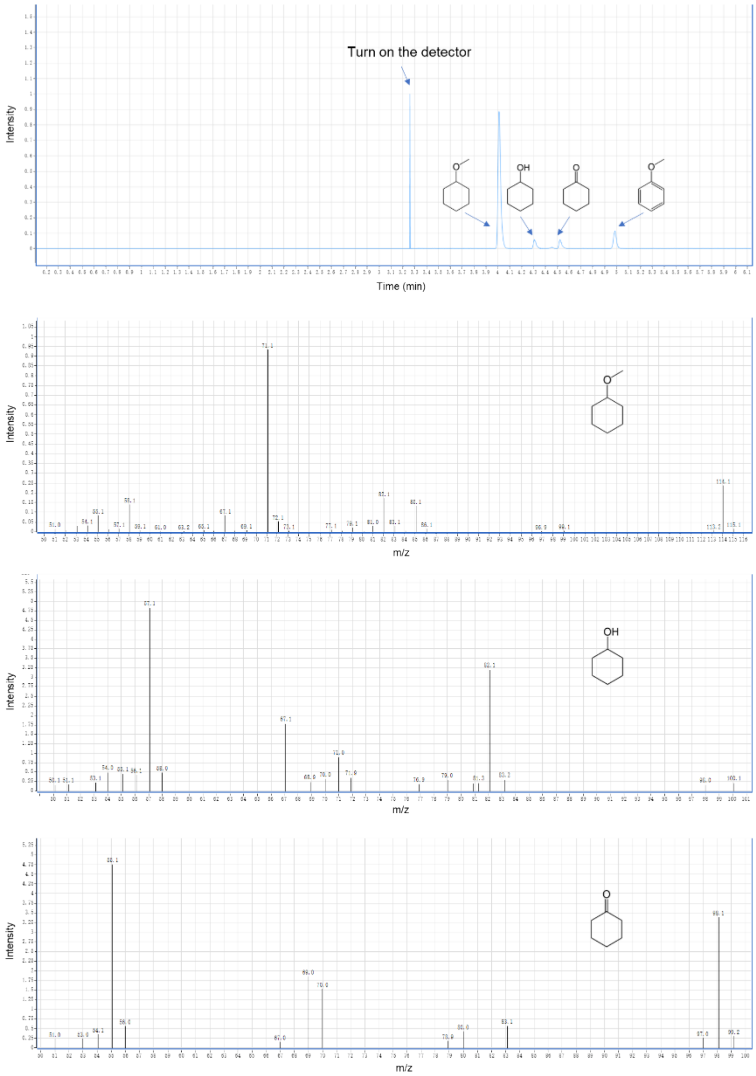

Figure S17. The original GC-MS spectra of products for ECH of anisole.

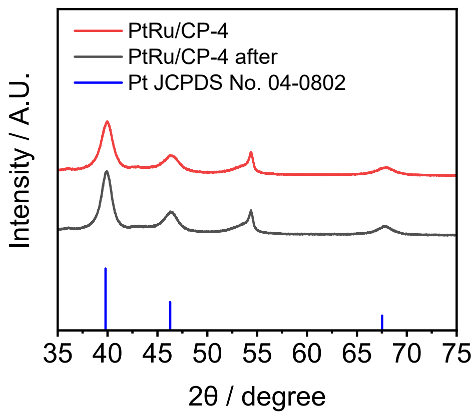

Figure S18. XRD patterns of fresh and 5-cycled PtRu/CP-4 catalyst.

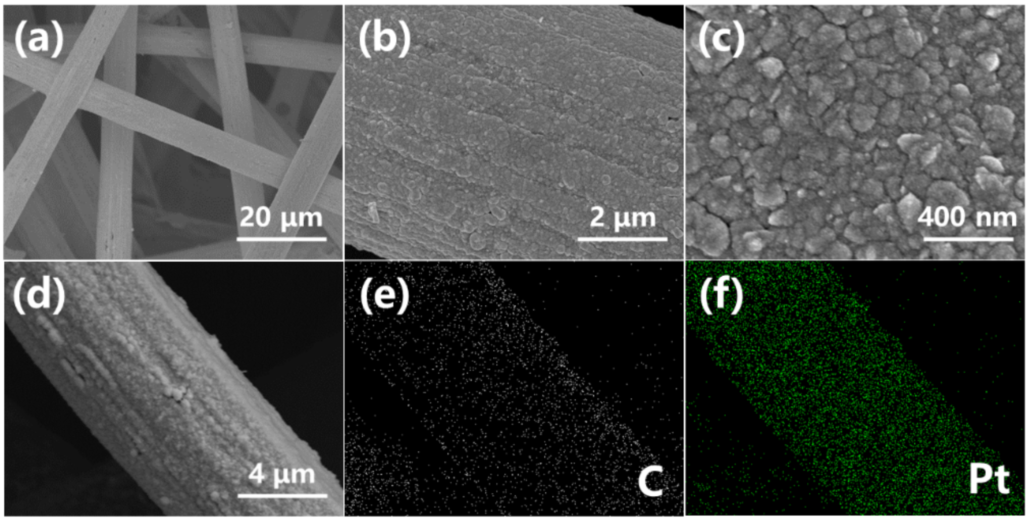

Figure S19. (a-c) SEM images for Pt/CP. (d-f) X-ray maps of C and Pt for Pt/CP.

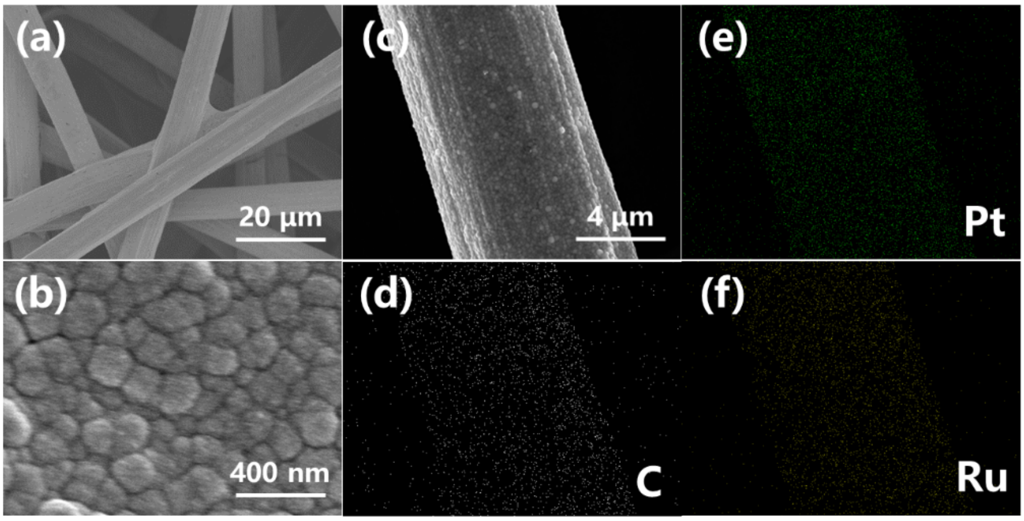

Figure S20. (a, b) SEM images for PtRu/CP-2. (c-f) X-ray maps of C, Pt, and Ru for PtRu/CP-2.

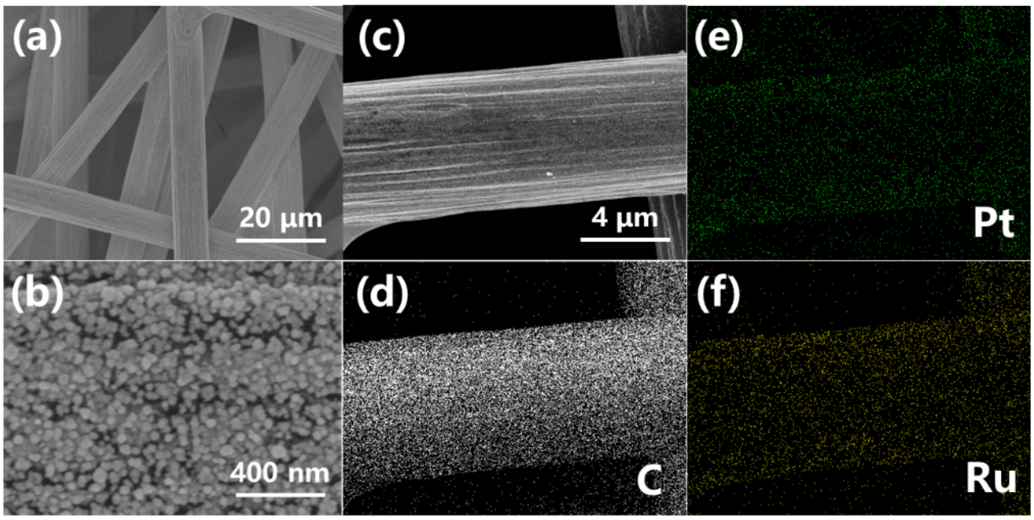

Figure S21. (a, b) SEM images for PtRu/CP-6. (c-f) X-ray maps of C, Pt, and Ru for PtRu/CP-6.

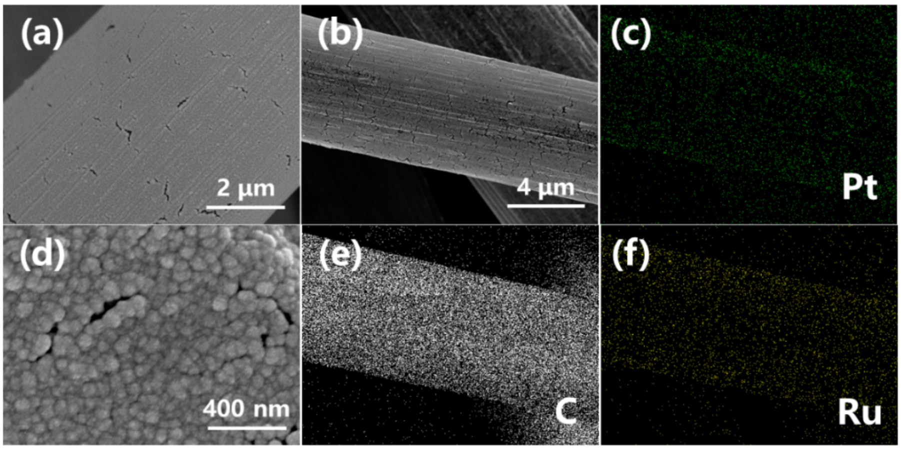

Figure S22. (a, b) SEM images for 5-cycled PtRu/CP-4. (c-f) X-ray maps of C, Pt, and Ru for 5-cycled PtRu/CP-4.

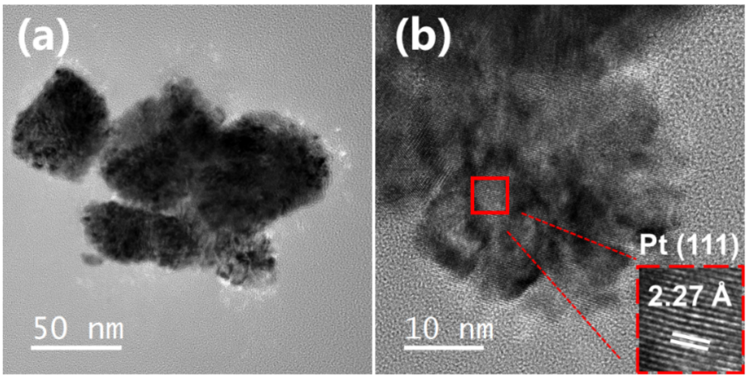

Figure S23. (a) TEM and (d) STEM image of Pt electrodeposited on CP.

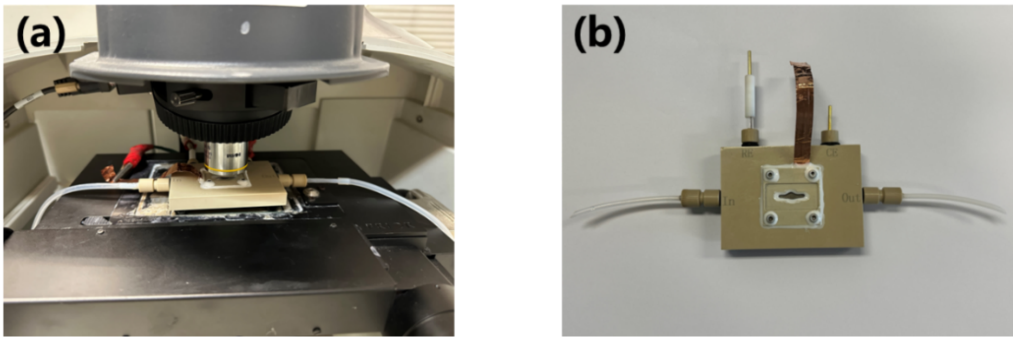

Figure S24. (a,b) Schematic diagram of the electrochemical cell for In situ Raman spectroscopy measurement.

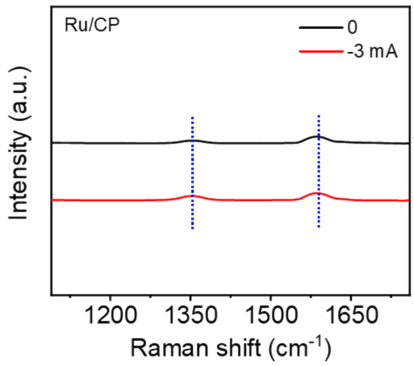

Figure S25. In-situ Raman spectra for Ru/CP at no current control and -3 mA. Condition: 0.2 M H_2SO_4, 10 mM BA.

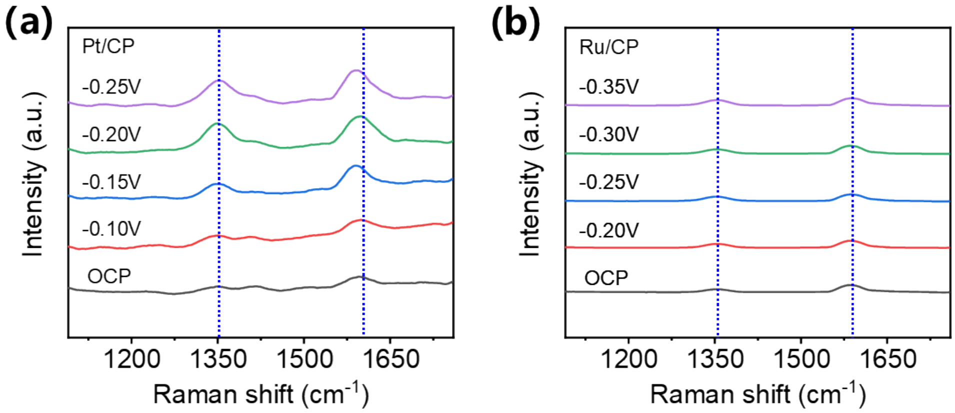

Figure S26. Potential-dependent Raman spectra for (a) Pt/CP and (b) Ru/CP under open circuit potential and different applied potentials (vs Ag/AgCl). Condition: 0.2 M H_2SO_4, 10 mM BA.

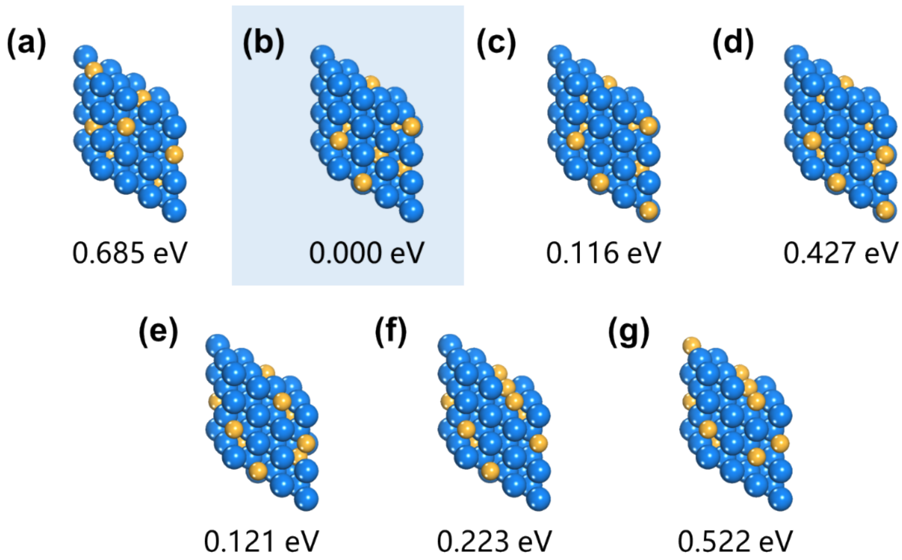

Figure S27. (a-g) Different configuration and relative energy of PtRu(111). Blue shading represents the most optimal structure.

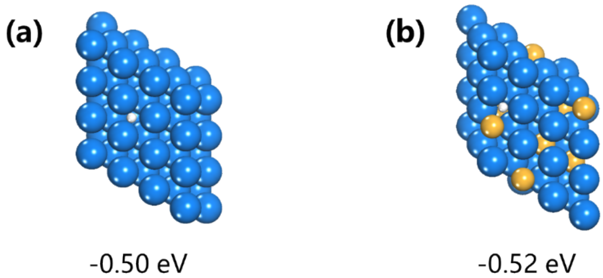

Figure S28. Adsorption configuration and energy of H atom over (a) Pt(111) and (b) PtRu(111).

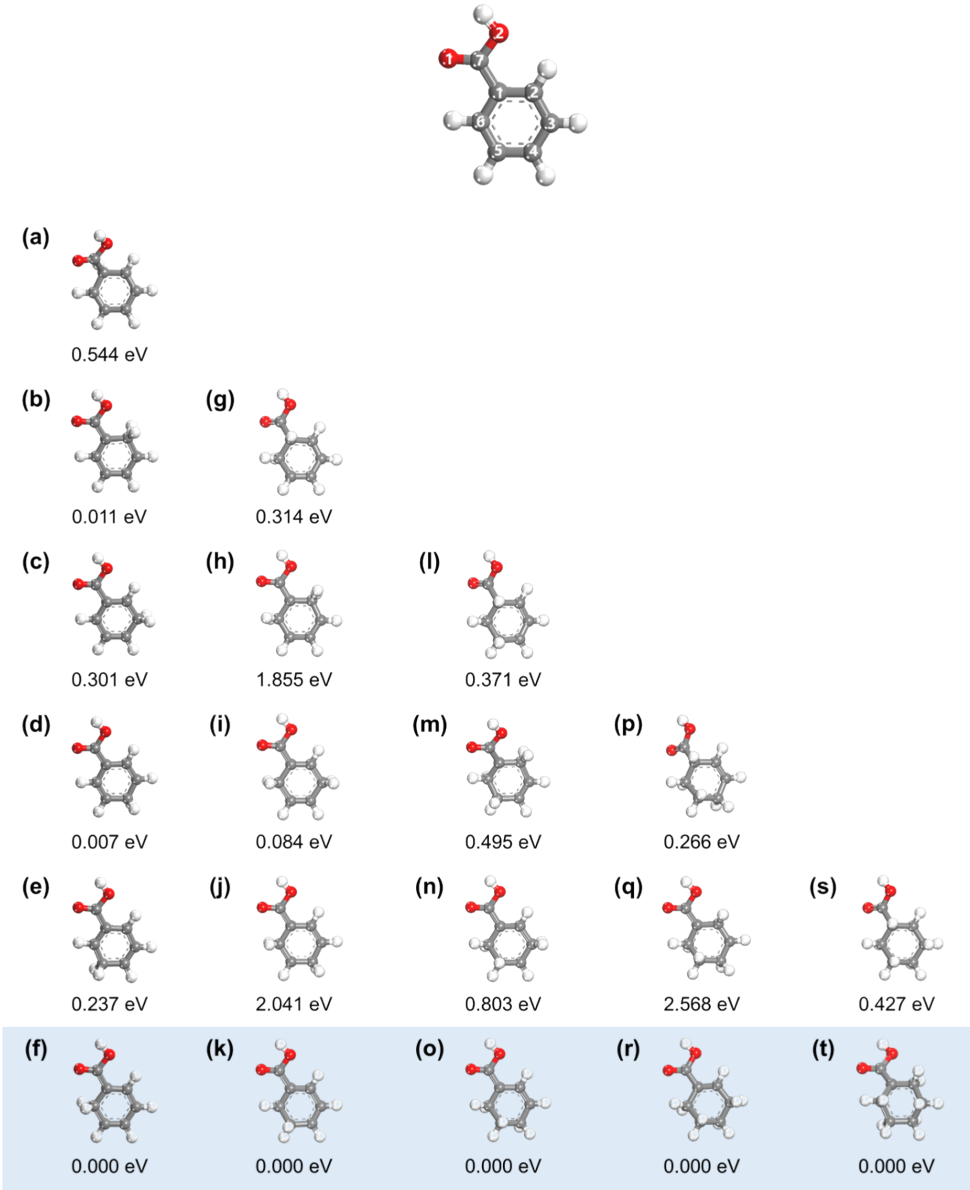

Figure S29. The optimized structure and relative energy of molecules obtained via one-by-one hydrogenation of BA. The grey, red, and white, atoms represent carbon, oxygen, and hydrogen respectively. The carbon atom is labeled with C_1 to C_7, and the oxygen atom is labeled with O_1 to O_2. Blue shading represents the hydrogenation sequence.

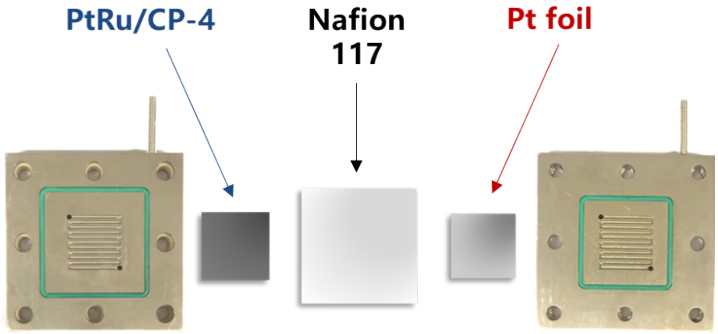

Figure S30. The photograph of the electrolyzer's internal structure.

Table S1. The potential using different catalysts after iR compensation (vs RHE).

	Pt/CP	Ru/CP	Pt/Ru/CP	PtRu/CP-2	PtRu/CP-4	PtRu/CP-6
η_{10}[a]	-0.038	-0.112	-0.038	-0.036	-0.037	-0.037
$\eta_{10\text{-}BA}$[b]	-0.032	-0.147	-0.031	-0.018	-0.017	-0.029
$\Delta\eta_{10}$[c]	0.006	-0.035	0.007	0.018	0.021	0.008

[a]η_{10} is measured in 0.2 M H_2SO_4 at -10 mA cm^{-2} current density.

[b]$\eta_{10\text{-}BA}$ is determined in 0.2 M H_2SO_4 containing 10 mM BA at -10 mA cm^{-2} current density.

[c]$\Delta\eta_{10}$ represents the difference between η_{10} and $\eta_{10\text{-}BA}$.

Table S2. The elemental ratio of Pt and Ru measured by SEM-EDX analysis and ICP-AES.

Catalyst	SEM-EDX	ICP-AES		
	mole ratio of Pt: Ru	Mass of Pt (mg)	Mass of Ru (mg)	mole ratio of Pt: Ru
Pt/CP		1.15		
PtRu/CP-2	6.94: 1	1.10	0.08	7.12: 1
PtRu/CP-4	5.58: 1	1.01	0.10	5.13: 1
PtRu/CP-6	3.62: 1	0.95	0.13	3.83: 1
Ru/CP			0.22	

Table S3. The different bond lengths of BA before and after adsorption on Pt(111) and PtRu(111).

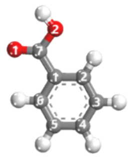

Bond	Benzoic acid/Å	Benzoic acid-Pt/Å	Benzoic acid-PtRu/Å
C_1-C_2	1.40	1.47	1.48
C_2-C_3	1.39	1.43	1.43
C_3-C_4	1.40	1.47	1.47
C_4-C_5	1.40	1.47	1.47
C_5-C_6	1.39	1.43	1.42
C_1-C_6	1.40	1.47	1.48
C_7-O_1	1.22	1.22	1.22
C_7-O_2	1.37	1.37	1.36